contrast to the mudstone and shale in the underlying Buckley Formation, but from about 300 m above the base of the Fremouw Formation at Graphite Peak, as at most other sections, the remains of stems (possibly *Neocalamites*) and roots are common. At the proposed type section (Fremouw Peak, central Queen Alexandra Range) 30 m below the top of the formation, the plant assemblage includes *Dicroidium odontopteroides* (*5*), indicating a Triassic age.

From the paleobotanical evidence an Early or Middle Triassic age for the bone-bearing strata is thought most likely, although a Late Permian age is possible.

The fragment of bone with which this report is concerned is not very large, being about 7 cm long, 3 cm high, and 2 cm wide. It is identified here as the back portion of the left mandibular ramus of a labyrinthodont amphibian.

The external surface of the bone, in this fragment composed of the surangular, is very rugose, with a pattern quite typical for a labyrinthodont. There are two discernible grooves with pits, one running from the dorsal edge of the bone forwardly and down, the other branching from this beneath the glenoid and running more or less horizontally to the front of the bone fragment. The obliquely directed groove is identifiable as the sulcus mandibularis, according to an earlier nomenclature (*6*), the other one being the sulcus oralis. The glenoid articulation of the articular bone is preserved on the outer surface of the bone; its inner portion is, however, missing. Along the ventral edge of the surangular, externally, is the squamous articulation for the angular bone.

There is a very large retroarticular process, partially preserved, and on the internal surface of this part of the bone are the lines of sutural articulation of the prearticular bone. At the very posterior edge of the bone fragment, internally, is a part of the foramen chorda tympani, evidently placed along the junction between the prearticular and surangular.

Anterior to the semicircular glenoid is the posteriormost part of the adductor fossa. This contains two, large, deep surangular foramina, in front of the glenoid and directed back beneath the articular. There is a small foramen lateral to each of these large foramina. This empirical description of the bone outlines briefly its salient osteological characters. The importance of the discovery of a Triassic tetrapod on the Antarctic continent can hardly be overemphasized. It bears upon the past relations of that continent to other southern land masses, as well as upon the zoogeographical relations of Triassic tetrapod faunas. Now, for the first time, there is direct evidence of land-living vertebrates inhabiting the Antarctic continent in a rather remote geologic period. And where one fragment has been found, there is every reason to think that, with diligent search, more fossils can be obtained.

In larger aspect, an assemblage of Antarctic Triassic tetropods, if found, will strengthen the evidence, now foreshadowed by this first discovery, of a land connection permitting Triassic tetrapods to migrate between Antarctica and some of the other southern continents. Its bearing upon the Triassic zoogeography of the Southern Hemisphere, and the very close affinities now recognized between the Triassic tetrapods of southern Africa and those of Brazil and Argentina, is obvious. Moreover, such an assemblage, if found, will be viewed against the background of Antarctic Gondwana plants (*7*).

PETER J. BARRETT
RALPH J. BAILLIE
Institute of Polar Studies, Ohio State University, Columbus 43210
EDWIN H. COLBERT
American Museum of Natural History and *Columbia University, New York*

References and Notes

1. G. W. Grindley, *New Zealand J. Geol. Geophys.* **6**, 307 (1963).
2. P. J. Barrett, D. H. Elliot, J. F. Lindsay, *Antarctic J. U.S.* **2**, 110 (1967).
3. F. A. Wade, V. L. Yeats, J. R. Everett, D. W. Greenlee, K. E. LaPrade, J. C. Schenk, *Texas Tech. Coll. Res. Rep. Ser. Antarctic Ser. No. 65–1* (1965), p. 24; D. H. Elliot and P. Tasch, *J. Paleontol.* **41**, 1561 (1967).
4. V. R. McGregor, *New Zealand J. Geol. Geophys.* **8**, 278 (1965).
5. J. F. Rigby and J. M. Schopf, in *Resumenes de trabajos presentados a las sesiones: Buenos Aires, Asoc. Geol. Argentina* (1967), abstr., p. 15 (International Symposium on Stratigraphy and Paleontology of the Gondwana, 1st, Mar del Plata, 1–4 Oct. 1967).
6. T. Nilsson, *K. Svenska Vetensk.-Akad. Handl.* **3**, bd. 20, No. 9 (1943); **3**, bd. 21, No. 1 (1944).
7. E. P. Plumstead, *Trans-Antarctic Exped. 1955–1958, Sci. Rep. No. 9* (1962) (Trans-Antarctic Exped. Comm., London).
8. Supported by grant No. GA-1159 from NSF to Ohio State University Research Foundation (RF 2494). The project is supervised by Dr. C. H. Summerson; Dr. J. M. Schopf reviewed the paleobotanical evidence. U.S. Naval Task Force 43 provided logistic support for the field work. Contribution No. 119 of the Institute of Polar Studies, Ohio State University, Columbus.

31 May 1968

Meteoroid Hazard near Moon

Abstract. *The meteoroid experiments by five Lunar Orbiters have provided direct measurements in the near-lunar environment of the rate of penetration of 0.025-millimeter beryllium copper by meteoroids. Each experiment used 20 pressurized-cell detectors having a total effective exposed area of 0.186 square meter. The spacecraft carrying the cells were in both equatorial and polar orbits; altitudes ranged between 30 and 6200 kilometers. Data collected continuously for 17 months indicate that the rate of penetration in the lunar environment is approximately half the rate in the near-Earth environment as measured by detectors of the same type aboard Explorers 16 and 23.*

Penetrations by meteoroids were measured by five Lunar Orbiters for assessment of the hazard to the pressurized camera system, and for comparison of the rate of penetration (of a metal skin) in the vicinity of Moon with rates measured near Earth. Such measurements would also help to determine the protection required for spacesuits, instruments, and spacecraft on the Apollo mission.

Estimates of the hazard near Moon have varied by several orders of magnitude; they have ranged from somewhat less to greater by several orders of magnitude than the hazard near Earth. A major uncertainty is the contribution by secondary meteoroids created by impacts of primary meteoroids on Moon.

Before the Lunar Orbiters the only measurements by satellites of meteoroid flux near Moon were made by Luna 10 with piezoelectric detectors that were sensitive to particle impacts; impacts were recorded at altitudes between 355 and 1050 km, the average rate of 4×10^{-3} m^{-2} sec^{-1} exceeding the average for interplanetary space by about two orders of magnitude (*1*).

The Lunar Orbiters carried pressurized-cell detectors like the ones flown near Earth aboard Explorers 16 and 23. Each is a pressurized semicylinder with a pressure-sensitive switch; the cylindrical surface of the detector is the test material, 0.025-mm beryllium copper. Gas pressure holds the switch closed, but when the pressure is released by puncture of the test material the switch returns to open and stays in this position as a permanent record

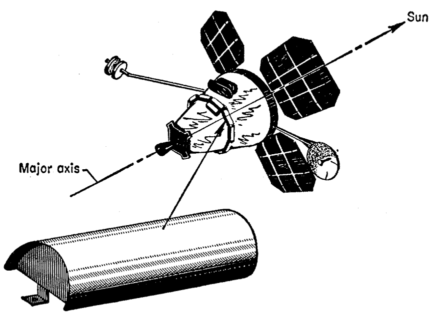

Fig. 1. Geometry of meteoroid detectors aboard spacecraft.

of the puncture. Whenever the condition of the detectors is telemetered, new punctures are indicated and previously indicated punctures are verified. Each spacecraft carried 20 of these detectors arranged in a ring around it (Fig. 1). Since 20 detectors could not be placed in a single ring, two were placed side by side in each of five positions on the ring. Each detector, being a semicylinder, shows half as much area when viewed from the side as when viewed from the top. When the ring is viewed from the small end of the spacecraft, along the major axis, the full ring of detectors is visible in side view. When the spacecraft is viewed from a direction normal to the major axis, the tops of approximately half the detectors are visible. Thus about the same area is presented in both directions.

The total area of the test material aboard each spacecraft was 0.282 m^2. Shielding by the solar-cell panels, antennas, and other components reduced this area by 34 percent, leaving an effective area of 0.186 m^2. Of course the shielding also compromised the isotropy of exposure of the test material to the environment.

The spacecraft was oriented with the large end, carrying the solar-cell panels, pointing toward Sun. The tapered midsection created a 20-deg-half-angle conical blind spot for the detectors in the direction of Sun, and the solar panels blocked about half the conical annulus between 20 and 60 deg. Since data were collected continuously for more than 1 year, the combined missions covered at least one complete orbit of Sun.

The average puncture rates were calculated by division of the total number of punctures by the total time-area product: $\psi = N/T$, where ψ is the puncture rate per square meter, per day; N is the total number of punctures; and T is the product of time (days) and area (square meters) of exposure. In determining the exposed time-area, one must consider the gradual loss in area as detectors are punctured; whenever a sensor is punctured, the effective area is reduced and the reduced area is effective until the next puncture.

Twenty-two punctures were recorded by the five Lunar Orbiters during a time-area exposure of 139.0 $m^2 \cdot$ day; the corresponding average rate of puncture was 0.16 m^{-2} day^{-1}. In addition, the detectors were exposed to 3.5 $m^2 \cdot$ day during transit between Earth and Moon, with no punctures. These data are compared (Table 1) with data collected from similar test material by Explorers 16 and 23 near Earth. Explorer 16 collected 44 punctures during a time-area exposure of 132.9 $m^2 \cdot$ day (0.33 m^{-2} day^{-1}), and Explorer 23 collected 50 punctures during exposure of 139.9 $m^2 \cdot$ day (0.36 m^{-2} day^{-1}). None of the data have been corrected for shielding of the spacecraft by Moon or Earth, but such shielding is about the same for all three experiments. Both the Lunar Orbiter and Explorer 23 periods covered at least 1 year, and the time-area exposures were almost the same.

Figure 2, a plot of rate of puncture as a function of thickness of test material, shows (i) the Lunar Orbiter average rate of puncture of 0.16 m^{-2} day^{-1}, with confidence limits (confidence coefficient, .95); (ii) the rates measured near Earth by Explorers 16 and 23 (*2, 3*); and (iii) Whipple's 1963 "best estimate" (*4*) converted to penetration rate (*3*).

The penetration rate measured by Lunar Orbiters was less by several orders of magnitude than that measured with piezoelectric sensors aboard Luna 10, interpreted in terms of rate of penetration. However, piezoelectric sensors have consistently indicated greater rates of meteoroid flux than have penetration detectors near Earth; one explanation could be the sensitivity of piezoelectric devices to noise of acoustic, thermal, or electrical origin (*5*).

Since the Lunar Orbiters were space-oriented, the distribution of punctures around them was examined for a possible predominant direction of the incoming flux. Reduction of data for the spacecraft's position has been completed for 11 of the 22 punctures; eight of these were on the side of the spacecraft that faced forward in the orbital direction of movement about Sun, and this preponderance agrees with Earth-based radar observations (*6*) indicating that the influx on the side of Earth facing forward (in orbit about Sun) is several times greater than influx on the opposite side. Corrections for the orbital velocity of Earth and the average velocity of meteors show (*6*) that the apparent directional characteristics of the influx are due to Earth's running into meteors on one side and running away from them on the opposite side. Although the radar data are for much larger meteoroids than would penetrate the detectors aboard the Lunar Orbiters, the penetration data do show the same general directional trend.

Estimates of the flux of secondary meteoroids near Moon indicate that it is great near the lunar surface but drops off sharply with altitude (*7*). The estimated velocities of particles, however, are typically lower than the velocities of primary meteoroids, so that any corresponding puncture hazard, or its variation with altitude, cannot be clearly estimated. The Lunar Orbiter penetration data were therefore examined for indication that the hazard varied with altitude.

Only eight of the 22 punctures occurred while the spacecraft's trans-

Table 1. Comparison of Lunar Orbiter data with data collected by Explorers 16 and 23 near Earth.

Spacecraft	Punctures	Exposure ($m^2 \cdot$ day)	Punctures (m^{-2} day^{-1})
Lunar Orbiters 1–5	22	139.0	0.16
Explorer 16	44	132.9	.33
Explorer 23	50	139.9	.36

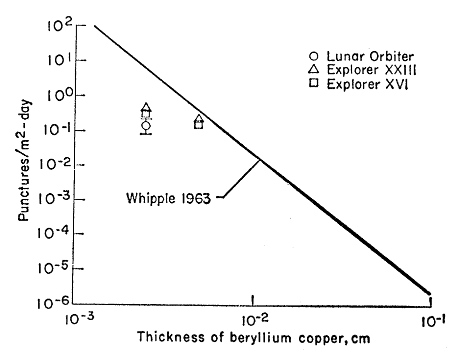

Fig. 2. Rates of puncture of pressurized cells of beryllium copper aboard Lunar Orbiter and Explorers 16 and 23; comparison with Whipple's 1963 prediction (modified for beryllium copper).

mitters were operating continuously; for the remainder the intervals between data readout were so long that the times of puncture, with the corresponding altitudes, could not be determined. For four of these eight punctures, which occurred while the spacecraft was occulted by Moon, the altitudes can be defined only within limits—the highest and lowest altitudes during the occultation periods. The altitudes at which the eight punctures occurred may then be 305 ± 120, 510 ± 200, 810 ± 90, 1125 ± 675, 1650, 1685, 5100, and 6040 ± 100 km. Study of these data, with due allowance for variation of residence time with altitude (the spacecraft spends less time near perilune than near apolune), indicated no statistically significant variation of hazard with altitude.

The difference between penetration rates near Moon and near Earth should probably be accepted as only tentative since (i) the number of penetrations is (statistically) fairly small, and (ii) the meteoroid flux in the neighborhood of Earth's orbit may vary from one measurement period to another. But the data do indicate with good confidence that the penetration hazard for 0.025-mm beryllium copper near Moon is no greater than near Earth. The data show no evidence of increase in the hazard that might result from secondary flux ("backsplash" from impacts of primary meteoroids on the lunar surface) in the altitude range between 30 and 6200 km. There was no apparent dependence on altitude, and the dependence on direction appeared to agree with that shown by Earth-based radar observations.

C. A. GURTLER
GARY W. GREW

Langley Research Center, National Aeronautics and Space Administration, Hampton, Virginia 23365

References

1. T. N. Nazarova, A. K. Rybakov, C. D. Komissarov, "Investigation of solid interplanetary matter in the vicinity of the moon," before 10th COSPAR meeting, London, July 1967.
2. E. C. Hastings, Jr., Ed., *NASA TM X-949* (March 1964).
3. R. L. O'Neal, Ed., *NASA TM X-1123* (August 1965).
4. F. L. Whipple, *J. Geophys. Res.* **68**(17), 4929 (1963).
5. G. P. Konstantinov, M. M. Bredov, Y. P. Mazets, "Experimental data against the hypothesis of a dust cloud around the earth," in *Rep. Acad. Sci. USSR* **174**(3) (1967); C. Nilsson, *Science* **153**, 1242 (1966).
6. G. S. Hawkins, *Monthly Notices Roy. Astron. Soc.* **116**(1), 92 (1956).
7. D. E. Gault, E. M. Shoemaker, H. J. Moore, *NASA TN D-1767* (1963).

24 June 1968

Tritium Enrichment by Gas-Solid Chromatography: Technique for Low-Level Analysis

Abstract. *A palladium chromatograph was developed that can detect less than 10 atoms of tritium per 10^{18} atoms of hydrogen. Columns operated at ambient temperature have 70-liter hydrogen capacity (50-milliliter water sample) and give 60 percent recovery in the first 500 cubic centimeters of gas evolved.*

Hydrogen isotopes can be separated in a chromatographic column filled with palladium black (*1*). I have developed a tritium-enriching chromatograph, based on this method of isotopic separation, that can detect 2 atoms of tritium (T) per 10^{18} atoms of hydrogen. This analytical system is simpler and faster than the electrolytic (*2*) or thermal-diffusion (*3*) techniques normally used. The technique is specific for tritium and unaffected by trace amounts of other radioactive isotopes.

The entire procedure, beginning with conversion of the water sample to hydrogen and ending with the 500-cm^3 enriched fraction in the proportional chamber, requires about 3.5 hours. Counting time varies with the level of sensitivity desired and with the background of the system; for my system (background of 6.4 count/min in a 2.6-liter chamber), a 30-minute counting period suffices for detection of original sample T:H concentrations greater than $1{:}10^{17}$ with an error (1σ) of 41 percent. Counting times up to 1000 minutes were used for radioassay of tritium concentrations below $1{:}10^{17}$.

Replicate analyses at T:H ratios from $4{:}10^{14}$ to $5{:}10^{17}$ (the lower concentration was restricted by availability of tritium-free water to make dilutions, and not by column characteristics) resulted in an overall recovery of 62 ± 6.3 percent at the 95 percent confidence level. There was no loss in recovery at the lower concentration.

If one assumes that recovery does not change for concentrations lower by at least one order of magnitude than those tested, Atlantic Ocean water had a T:H ratio of $2{:}10^{17}$, and Savannah River water, stored in glass, contained 1.3 atoms of tritium per 10^{17} atoms of hydrogen. Both results compare favorably with published values (*4*). The lowest tritium concentration was found in deep-well water freshly sampled and quickly processed before significant exchange with atmospheric water could occur; the estimated initial T:H ratio of $2{:}10^{18}$ increased to $2.0{:}10^{17}$ after storage for 6 months at room temperature in a capped polyethylene bottle—because of infusion and exchange of tritium from moisture in ambient air (T:H, $3{:}10^{15}$). The lowest atomic T:H concentration previously tested for enrichment characteristics, by a chromatographic system, was $1{:}10^{14}$ (*5*); a molecular-sieve column was used at liquid-nitrogen temperature. The capacity of this column was later increased from 300 ml of hydrogen to 10 liters (*6*), but behavior at low concentrations was not reported.

The enrichment scheme is as follows: The water sample is reacted with magnesium chips at 650°C. The hydrogen generated sorbs directly onto an evacuated palladium column. When a sufficient volume of water has reacted, the furnace is isolated and cooled. No buffer gas or carrier gas is used; movement of hydrogen through the column is maintained by the initial pressure

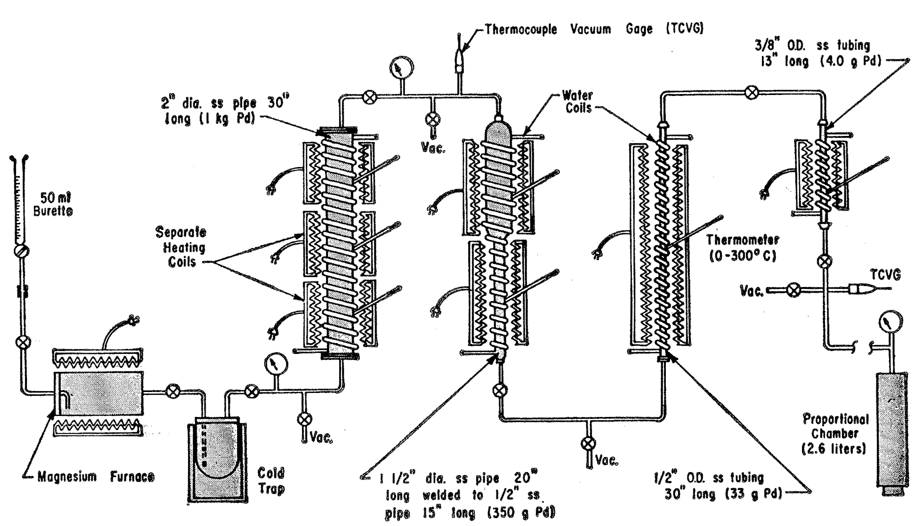

Fig. 1. Experimental arrangement of palladium columns (diagrammatic).